Int. J. Multiphase Flow Vol. 19, No. 3, pp. 421–437, 1993
Printed in Great Britain

0301-9322/93 $6.00 + 0.00
Pergamon Press Ltd

PRESSURE PROFILES FOR SLUGS IN HORIZONTAL PIPELINES

Z. FAN, Z. RUDER and T. J. HANRATTY
Department of Chemical Engineering, University of Illinois, Urbana, IL 61801, U.S.A.

(Received 1 October 1991; in revised form 10 February 1993)

Abstract—Measurements are presented of the variation of pressure caused by the passage of a stable or unstable slug in a horizontal gas–liquid flow. Good agreement is obtained with a model which considers the pressure change as the sum of contributions from a hydraulic jump in the front of the slug, the wall drag in the body of the slug and a sudden change in the velocity of the liquid in the rear of the slug.

Key Words: slug flow, gas–liquid flow, horizontal pipelines, pressure profiles, model for slugs

1. INTRODUCTION

The slug pattern that is observed for gas–liquid flow in horizontal pipes is characterized by the intermittent appearance of highly aerated slugs of liquid. The large pressure pulsations that accompany slugs have been used by a number of researchers (Dukler & Hubbard 1975; Weisman *et al.* 1979; Lin & Hanratty 1986, 1987) to detect their existence. The usefulness of this approach is clearly demonstrated in the experiments of Lin & Hanratty, which show that the arrival of a slug at a location in a pipe is accompanied by a sudden increase in both the liquid level and the pressure. This implies that there would be a discontinuous increase in pressure over each one of the slugs in the pipeline.

These type of results suggest that a general method to predict the overall pressure drop should be developed from an understanding of the behavior of individual slugs and a prediction of the number of slugs in a given length of pipe. This paper presents results on the pressure variation over single slugs, which are needed to develop such a model.

Experiments were carried out in a horizontal pipeline with an inside diameter of 0.095 m. A piezoresistive pressure transducer, mounted flush to the top wall of the pipe, was used to measure the pressure variation as a slug passes. The void fraction, the velocity, the length of individual slugs and the liquid height in front of and behind the slugs were measured with two pairs of conductance wires.

In 1970, Singh & Griffith proposed a model for the pressure drop over single slugs which identified three contributions:

$$\Delta\tilde{P}_T = \Delta\tilde{P}_m + \Delta\tilde{P}_f + \Delta\tilde{P}_g, \qquad [1]$$

where $\Delta\tilde{P}_T$ is the total pressure drop over a single slug, $\Delta\tilde{P}_m$ is the pressure drop due to the mixing of the liquid in the front of the slug, $\Delta\tilde{P}_f$ is the pressure drop caused by the frictional drag at the pipe wall and $\Delta\tilde{P}_g$ is the pressure drop needed to balance the gravitational force in an inclined pipe. Beggs & Brill (1973) presented an equation to calculate the pressure drop over slugs based on an energy balance. Bonnecaze *et al.* (1971) first proposed a theoretical model for the pressure drop across a single slug by using a reference frame moving at the slug translational velocity, C_F. Dukler & Hubbard (1975) pictured the liquid slugs as sustaining itself by scooping up liquid from the carpet in its front and shedding the liquid at its tail. The thickness of the liquid carpet and the velocity of the slug emerge from this analysis as parameters of great importance. Dukler & Hubbard identified the irreversible acceleration of the liquid picked up by the slug as the largest contributor to pressure pulsations. Kokal & Stanislav (1989) and Crowley (1989) used an analysis similar to what was proposed by Singh & Griffith (1970) and Dukler & Hubbard (1975).

The results presented in this paper are interpreted with a model developed by Ruder *et al.* (1989) and Ruder & Hanratty (1990) to establish general conditions for the existence of slugs. It is quite

similar to the suggestions by Singh & Griffith (1970) and Dukler & Hubbard (1975). The papers by Ruder and coworkers were motivated by the failure of linear stability analyses of stratified flows to account for observations of the initiation of slug flow for a number of experimental conditions. They suggested that the stability of a slug requires that the height of the liquid carpet in the front of the slug has a certain critical value. When it is larger than the critical value, the rate of accumulation of liquid into the slug exceeds the rate at which liquid is shed from the tail, so the slug grows. If it is smaller than the critical value, the slug will decay because liquid is lost from the tail at a greater rate than it can be accumulated in the front.

The model considers the front of a slug as a one-stage sudden expansion (or as a hydraulic jump) and the back as an inviscid bubble of the type described by Benjamin (1968). It is supported both by photographic studies and by measurements of the height of the liquid layer in front of stable slugs. The principal problem in using it to interpret measurements of the pressure profile is to account for the effect of aeration. A simplifying assumption is made in this paper that the occluded air in the front part of the slug is moving at the same velocity as the liquid in the slug and is behaving as if it were uniformly distributed.

2. THEORY

Figure 1 presents a simple picture of a slug. For gas/liquid flow in a horizontal pipe, the pressure drop over the slug is considered as being composed of three parts: the change associated with the hydraulic jump in front of the slug from stations 1 to 3, $\Delta\tilde{P}_h$; a frictional loss in the body of the slug from stations 3 to 4, $\Delta\tilde{P}_f$; and a pressure variation associated with the velocity change at the rear of the slug from stations 4 to 5, $\Delta\tilde{P}_r$. Thus, the total pressure change is given as

$$\Delta\tilde{P}_T = \Delta\tilde{P}_h + \Delta\tilde{P}_f + \Delta\tilde{P}_r. \quad [2]$$

The front of the slug is moving downstream with a velocity C_F. The liquid and gas velocities at locations 1, 3 and 4 are uniform; they are represented by u_{Li} and u_{Gi}, respectively. The liquid layer in front of the slug, which has a velocity u_{L1} in a laboratory framework, is devoid of air. The flows of the liquid and gas in the slug body are uniform after a short distance behind the slug front and have the same velocity, $u_{G3} = u_{L3}$. The gas is uniformly distributed in the body of the slug between stations 3 and 4.

2.1. Pressure Drops at the Front and Rear of a Slug

2.1.1. Stable slugs

Consider a frame of reference moving with velocity C_F. A control volume is chosen from stations 1 to 3. Since a positive velocity is defined as the direction in which the slug is moving in a laboratory framework, the velocities in and out of the slug at stations 1 and 3, in the moving reference frame, have negative values and are designated by $-(C_F - u_{Li})$ and $-(C_F - u_{Gi})$.

Conservation of mass for the liquid between stations 1 and 3 gives

$$(C_F - u_{L1})A_{L1} = (C_F - u_{L3})A_3(1 - \epsilon_3). \quad [3]$$

Conservation of mass for the gas gives

$$(C_F - u_{G1})(A_3 - A_{L1}) = (C_F - u_{G3})A_3\epsilon_3 = R_A. \quad [4]$$

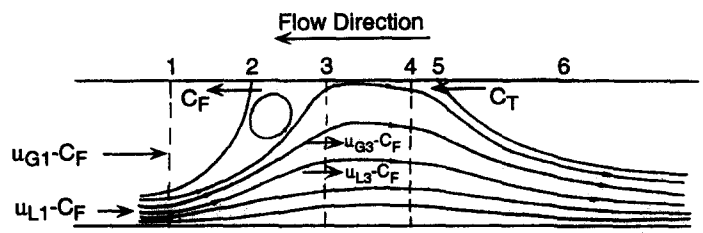

Figure 1. Definition of variables for a slug in the reference frame moving with velocity C_F.

Here, A_{L1} is the area of the liquid layer in front of the slug, A_3 is the pipe cross-sectional area, R_A is the rate at which air is occluded into the slug and ϵ_3 is the void fraction in the slug body.

The length between stations 1 and 2 is assumed small enough so that the resisting stress at the pipe wall is neglected. (The error in this assumption is compensated for, to some extent, because the whole length of the slug is used in calculating the pressure drop due to wall friction.) Conservation of momentum gives

$$\tilde{P}_1 A_3 + \rho_L (C_F - u_{L1})^2 A_{L1} + \rho_G (C_F - u_{G1})^2 (A_3 - A_{L1}) + \rho_G g (A_3 - A_{L1}) h_{G1}^C + \rho_L g A_{L1} h_{L1}^C$$
$$= \tilde{P}_3 A_3 + \rho_L (C_F - u_{L3})^2 A_3 (1 - \epsilon_3) + \rho_G (C_F - u_{G3})^2 A_3 \epsilon_3 + [\rho_G \epsilon_3 + \rho_L (1 - \epsilon_3)] g A_3 h_3^C, \quad [5]$$

where $\tilde{P}_1$ and $\tilde{P}_3$ are the pressures at the top of the pipe, ρ_L and ρ_G are the densities of the liquid and the gas, h_{L1}^C, h_{G1}^C and h_3^C are, respectively, the centroid heights for hydrostatic pressure in the liquid layer, the air pocket in front of the slug and and the slug body. They may be viewed as a length scale that gives the average hydrostatic pressure over the area being considered. The pressure drop caused by the hydraulic jump in front of the slug is obtained by substituting [3] and [4] into [5]:

$$\frac{\Delta \tilde{P}_h}{\rho_L g} = \frac{1}{g}\left[\frac{A_{L1}}{A_3} - \left(\frac{A_{L1}}{A_3}\right)^2 \frac{1}{1 - \epsilon_3}\right](C_F - u_{L1})^2 + \left[\frac{A_{L1}}{A_3} h_{L1}^C - (1 - \epsilon_3) h_3^C\right]$$
$$+ \frac{\rho_G}{\rho_L g}\left[\left(1 - \frac{A_{l1}}{A_3}\right)(C_F - u_{G1})^2 - \epsilon_3 (C_F - u_{G3})^2\right] + \frac{\rho_G}{\rho_L}\left[h_{L2}^C \left(1 - \frac{A_{L1}}{A_3}\right) - \epsilon_3 h_3^C\right], \quad [6]$$

where $\Delta \tilde{P}_h = \tilde{P}_3 - \tilde{P}_1$. The last two terms in [6] are very small compared to the first two because ρ_G / ρ_L is a small number.

For a stable slug the velocity of the tail, C_T, is equal to C_F. The pressure change in the rear is approximated by assuming that, in a frame of reference moving with velocity C_F, the rear may be pictured as a Benjamin bubble. As shown by Ruder *et al.* (1989), this requires that the top of the slug tail is a stagnation point and that the pressure change associated with the acceleration (in reference frame C_F) along the top wall can be calculated from the Bernoulli equation. Because surface tension effects are negligible, the pressure in the liquid at the top of the tails equals the gas pressure, P_6. Thus, a pressure increase is calculated between stations 4 and 6 as

$$\Delta \tilde{P}_r = \tilde{P}_6 - \tilde{P}_4 = \tfrac{1}{2} \rho_L (C_F - u_{L4})^2, \quad [7]$$

where $u_{L4} = u_{L3}$.

2.1.2. *Unstable slugs*

For a growing slug, $C_F > C_T$, the length of the slug is increasing and the reference frame is chosen to move with velocity C_F. Station 1 moves with velocity C_F. Stations 3 and 4 are chosen to move with a velocity C_T so that the steady-state Bernoulli equation can be used between stations 4 and 5. The control volume between stations 1 and 3 extends in length at a rate $C_F - C_T$, which is equal to the rate at which the whole slug increases its length. The velocities in the reference frame at stations 1, 3 and 5 are, respectively, $-(C_F - u_{L1})$, $-(C_F - u_{l3})$ and $-(C_F - C_T)$. The tail of the slug is not a stagnation point.

The mass balance for the liquid phase from stations 1 to 3 is

$$(C_F - u_{L1}) A_{L1} = (C_F - u_{L3}) A_3 (1 - \epsilon_3) + (C_F - C_T) A_3 (1 - \epsilon_3). \quad [8]$$

The last term in [8] is the accumulation of liquid within the control volume. The following relation can be obtained from [8]:

$$(C_F - u_{L3}) = \frac{1}{(1 - \epsilon_3)}\left(\frac{A_{L1}}{A_3}\right)(C_F - u_{L1}) - (C_F - C_T). \quad [9]$$

If the momentum of the gas phase is neglected, the momentum balance is

$$\tilde{P}_1 A_3 + \rho_L (C_F - u_{L1})^2 A_{L1} + \rho_L g A_{L1} h_{L1}^C = \tilde{P}_3 A_3 + \rho_L (C_F - u_{L3})^2 A_3 (1 - \epsilon_3)$$
$$+ \rho_L (1 - \epsilon_3) g A_3 h_3^C + \rho_L A_3 (1 - \epsilon_3)(C_F - C_T)(C_F - u_{L3}), \quad [10]$$

where, again, the last term is the accumulation of momentum within the control volume. By substituting [9] into [10], it is found that

$$\frac{\Delta\tilde{P}_h}{\rho_L g} = \frac{1}{g}\left[\frac{A_{L1}}{A_3} - \left(\frac{A_{L1}}{A_3}\right)^2 \frac{1}{(1-\epsilon_3)}\right](C_F - u_{L1})^2 - \frac{1}{g}\left(\frac{A_{L1}}{A_3}\right)(C_F - C_T)(C_F - u_{L1}) + \left[\left(\frac{A_{L1}}{A_3}\right)h_{L1}^C - (1-\epsilon_3)h_3^C\right]. \quad [11]$$

The pressure drop at the rear of the slug is

$$\Delta\tilde{P}_r = \tilde{P}_5 - \tilde{P}_4 = \tfrac{1}{2}\rho_L[(C_F - u_{L3})^2 - (C_F - C_T)^2]. \quad [12]$$

By substituting [9] into [12], the following relation is obtained:

$$\Delta\tilde{P}_r = \frac{1}{2}\rho_L \frac{1}{(1-\epsilon_3)}\left(\frac{A_{L1}}{A_3}\right)(C_F - u_{L1})\left[\left(\frac{A_{L1}}{A_3}\right)\left(\frac{1}{1-\epsilon_3}\right)(C_F - u_{L1}) - 2(C_F - C_T)\right]. \quad [13]$$

Usually, $(C_F - u_{L3})$ is very small. When $(C_F - C_T)$ is larger than $(C_F - u_{L3})$, the pressure drop at the rear of the growing slug is negative.

For decaying slugs, $C_F < C_T$, the reference frame is chosen to move at the velocity C_T, so that the fluid in the different parts of the slug move in the same direction. Station 1 moves with velocity C_F and stations 3 and 4 are chosen to move with velocity C_T. The length of the control volume between stations 1 and 3 changes at a rate $C_F - C_T$. The flow at the top of the slug tail is a stagnation point.

The following relations are obtained:

$$C_F - u_{L3} = \frac{1}{(1-\epsilon_3)}\left(\frac{A_{L1}}{A_3}\right)(C_T - u_{L1}) \quad [14]$$

and

$$\frac{\Delta\tilde{P}_h}{\rho_L g} = \frac{1}{g}\left[\frac{A_{L1}}{A_3} - \left(\frac{A_{L1}}{A_3}\right)^2 \frac{1}{(1-\epsilon_3)}\right](C_T - u_{L1})^2 - \frac{1}{g}\left(\frac{A_{L1}}{A_3}\right)(C_F - C_T)(C_T - u_{L1}) + \left[\left(\frac{A_{L1}}{A_3}\right)h_{L1}^C - (1-\epsilon_3)h_3^C\right]. \quad [15]$$

The pressure drop at the slug rear is

$$\Delta\tilde{P}_r = \tilde{P}_5 - \tilde{P}_4 = \tfrac{1}{2}\rho_L(C_T - u_{L3})^2 = \tfrac{1}{2}\rho_L\left[\frac{1}{(1-\epsilon_3)}\left(\frac{A_{L1}}{A_3}\right)(C_T - u_{L1}) - (C_F - C_T)\right]^2. \quad [16]$$

For a decaying slug, $\Delta\tilde{P}_r$ is always positive, as is the case for a stable slug.

2.2. The Pressure Drop Due to the Frictional Drag in the Slug Body

The pressure drop in the body of the slug is pictured as mainly resulting from the frictional drag at the wall, so that

$$\Delta\tilde{P}_f = \tilde{P}_4 - \tilde{P}_3 = \tau_W \pi \frac{DL_S}{A_3}, \quad [17]$$

where τ_W is the average resisting stress at the wall and L_S is the length of the slug. Because of a lack of better information, the wall stress is approximated with the Blasius equation,

$$\tau_W = 0.046\left(\frac{D}{\nu_L}\right)^{-0.20}\frac{\rho_L}{2}u_{L3}^{1.8}, \quad [18]$$

where ν_L is the kinematic viscosity of the liquid. In [18], ρ_L is chosen as the effective density for the reasons cited in Fan *et al.* (1991). The lengths of the individual slugs are not given by the theory. They were obtained from measurements of the slug velocity and the time required for the slug to pass a measuring station.

2.3. *Estimation of u_{L1} and u_{L3}*

In the experiments, the height of the liquid layer in front of the slug, h_{L1}, is measured by conductance probes. The velocity u_{L1} is estimated by assuming the wavy layer is the same as a fully developed stratified flow. The errors introduced by this assumption are not serious since the calculations of the pressure drop over a slug are not sensitive to the value of u_{L1}.

The momentum balances for a stratified flow at station 1 are:

$$-(A_3 - A_{L1})\left(\frac{d\tilde{p}}{dx}\right) - \tau_{WG} S_G - \tau_{int} S_{int} = 0, \quad [19]$$

for the gas phase; and

$$-A_{L1}\left(\frac{d\tilde{p}}{dx}\right) - \tau_{WL} S_L + \tau_{int} S_{int} = 0, \quad [20]$$

for the liquid phase; where τ_{WG} and τ_{WL} are the resisting stresses at the pipe wall in contact with the gas and in contact with the liquid, τ_{int} is the shear stress at the interface, S_G and S_L are perimeters of the gas and the liquid at the pipe wall and S_{int} is the width of the interface of the liquid layer. By eliminating (dp/dx) between [19] and [20], the following equation for τ_{WL} can be obtained:

$$\tau_{WL} = \tau_{WG}\left[\frac{S_G A_{L1}}{S_L(A_3 - A_{L1})}\right] + \tau_{int}\frac{S_{int}}{S_L}\left[1 + \frac{A_{L1}}{(A_3 - A_{L1})}\right]. \quad [21]$$

The stresses τ_{WG} and τ_i are calculated by using the relations

$$\tau_{WG} = f_G \frac{\rho_G u_{G1}^2}{2} \quad [22]$$

and

$$\tau_{int} = f_{int} \frac{\rho_G u_{G1}^2}{2}. \quad [23]$$

Andritsos & Hanratty (1987) suggest

$$f_G = 0.046\, \mathrm{Re}_G^{-0.2} \quad [24]$$

and

$$\frac{f_{int}}{f_G} = \begin{cases} 1, & \text{for } u_{G1} < 5 \text{ m/s} \\ 1 + 15\left(\dfrac{h_{L1}}{D}\right)^{0.5}\left(\dfrac{u_{G1}}{5} - 1\right) & \text{for } u_{G1} < 5 \text{ m/s} \end{cases},$$

where u_{G1} is given in m/s.

After τ_{WL} is calculated, the characteristic stress in the liquid is taken as

$$\tau_c = \tfrac{2}{3}\tau_{WL}\left(1 - \frac{h_{L1}}{D}\right) + \tfrac{1}{3}\tau_i. \quad [25]$$

The friction velocity and the dimensionless liquid height are defined as

$$u_c^* = \left(\frac{\tau_c}{\rho_L}\right)^{0.5} \quad [26]$$

and

$$h^+ = \frac{h u_c^*}{\nu_L}. \quad [27]$$

Then, with the equation suggested by Andritos & Hanratty (1987),

$$h^+ = \left\{(1.082\, \mathrm{Re}_L^{0.5})^5 + \left[\frac{0.098\, \mathrm{Re}_L^{0.85}}{\left(1 - \dfrac{h_{L1}}{D}\right)^{0.5}}\right]^5\right\}^{0.2}, \quad [28]$$

Re_L and u_{L1} can be obtained, since h_{L1} is known.

When calculating the pressure drop due to the frictional drag at the pipe wall, u_{L3} must be known. This is obtained by using the mass balance equations:

for stable slugs, according to [3],

$$u_{L3} = C_F - \frac{1}{(1-\epsilon_3)}\left(\frac{A_{L1}}{A_3}\right)(C_F - u_{L1}); \quad [29]$$

for growing slugs, according to [9],

$$u_{L3} = 2C_F - \frac{1}{(1-\epsilon_3)}\left(\frac{A_{L1}}{A_3}\right)(C_F - u_{L1}) - C_T; \quad [30]$$

and

for decaying slugs,

$$u_{L3} = C_F - \frac{1}{(1-\epsilon_3)}\left(\frac{A_{L1}}{A_3}\right)(C_F - u_{L1}). \quad [31]$$

2.4. Calculated Results

Measured pressure profiles are compared with the pressure drops calculated from [6], [7] and [18] for stable slugs and from [6], [13] and [18] for unstable slugs. These calculations used measurements of h_{L1}, C_F, $(C_F - C_T)$, L_S and ϵ_3. Velocity u_{G1} was estimated as $u_{GS}\,A/A_{G1}$. Velocity u_{L1} was obtained from the stratified flow model and u_{L3} from [29], [30] and [31]. No attempts were made to develop models for C_F, L_S or ϵ_3.

3. EXPERIMENTS

The test pipeline had a length of 24 m and a design similar to that used by Laurinat *et al.* (1984). An important change, however, was made at the entrance section. The simple pipe tee mixer was replaced by a box, with dimensions of 0.494 × 0.434 × 0.381 m. The liquid was introduced into the box at its lower part and the air, at the upper part. The exit from the box consisted of a circular pipe that was attached to a side that was 0.434 m high and 0.381 m wide. The gas and liquid flowed out of the box in a stratified pattern and the liquid level inside the box fixed the liquid height at the entrance to the pipeline. Depending on the flow conditions, a slug is initiated at different positions in the pipe.

The height of the stratified liquid layer between slugs was measured with conductance probes, as described elsewhere (Laurinat *et al.* 1984; Lin & Hanratty 1987; Ruder *et al.* 1989). Platinum wires with a small diameter of 0.254 mm were used so that disturbances introduced into the gas and liquid flows would be small. The calibration for the stratified flow in figure 2 (designated by the points for a separate flow) was developed by measuring the ratio of the conductance when the pipe is partially filled to the value obtained when the pipe was completely filled with water. The normalizing conductance varied from day to day, so it was determined before each experiment.

The liquid fraction inside a slug was also estimated from conductance measurements. For a case in which bubbles are uniformly distributed over the pipe cross section the conductance ratio is equal to the liquid fraction, $(1 - \epsilon_3)$, as indicated in figure 2 by the points for a uniform flow. Visual observations suggested that, when the translational velocity of the slug is high, the bubbles are uniformly distributed along the whole length of the slug. However, when the translational velocity of the slug is low, the bubbles are uniformly distributed across the pipe section only in the front part of the slug; they are buoyed to the upper part of the pipe at the rear of the slug to give a configuration close to a separated flow. For the studies discussed in this paper, very little change of conductance was observed as the slug passed, so the uniform flow model was assumed to be applicable. Figure 3 compares measured void fractions with a correlation developed by Gregory *et al.* (1978).

Two pairs of probes separated by 0.254 m were used in these measurements. The velocity of the slug could then be determined by measuring the time required for the slug to move between these two measuring stations.

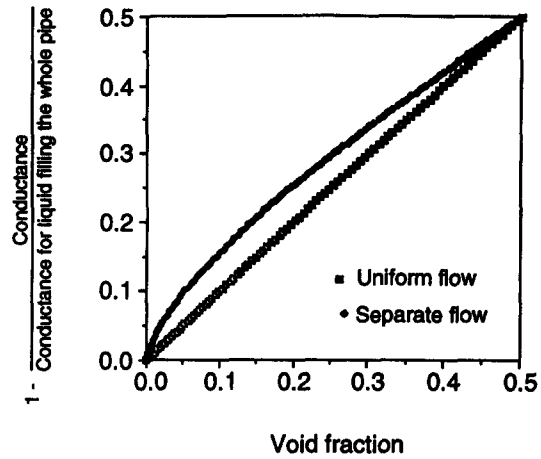

Figure 2. Comparison of calibrations of conductance for different liquid configurations.

The pressure profiles associated with the passage of a slug were measured by a piezoresistive pressure transducer, model 8510B-5 from ENDEVCO. The resonant frequency of this transducer is 85 kHz, which is high enough to pick up the characteristics of the pressure profiles. The pressure transducer was mounted flush to the top wall of the pipe to keep time delays as small as possible. Because the diameter of the pressure transducer is small (4 mm), it fits the inside wall of the pipe very well and does not produce any disturbances to the flow.

The conductance probes and the pressure transducer were contained in a test section, shown in figure 4, that was located 21 m from the entrance of the pipeline. The signals from the conductance probes and the pressure transducer were amplified, digitized and stored on an IBM computer. The sampling frequency of each channel varied from 0.5 to 1.5 kHz and depended on the gas velocity.

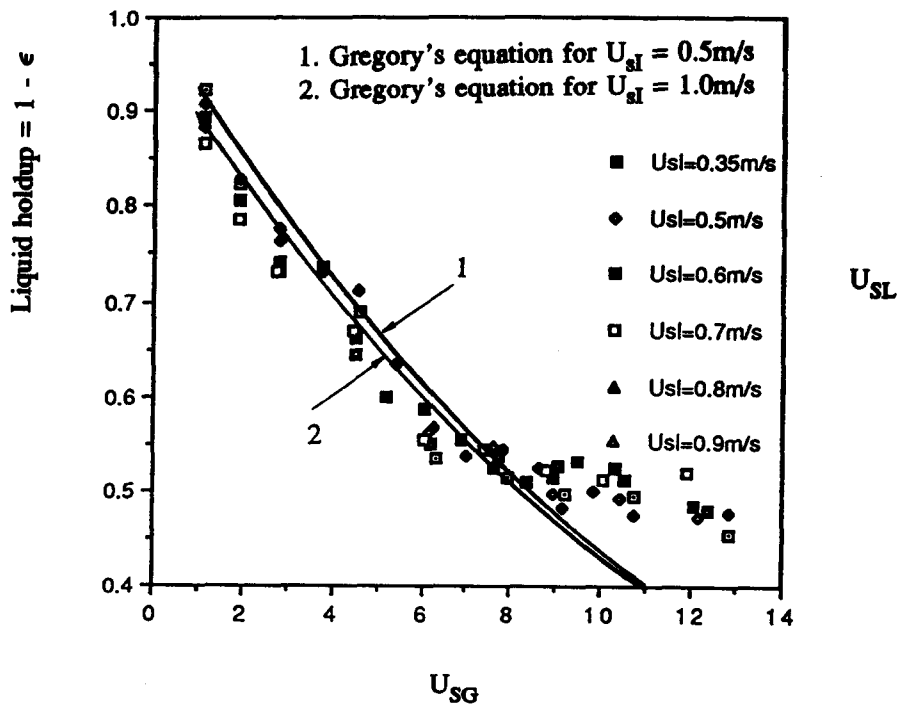

Figure 3. Void-fraction measurements.

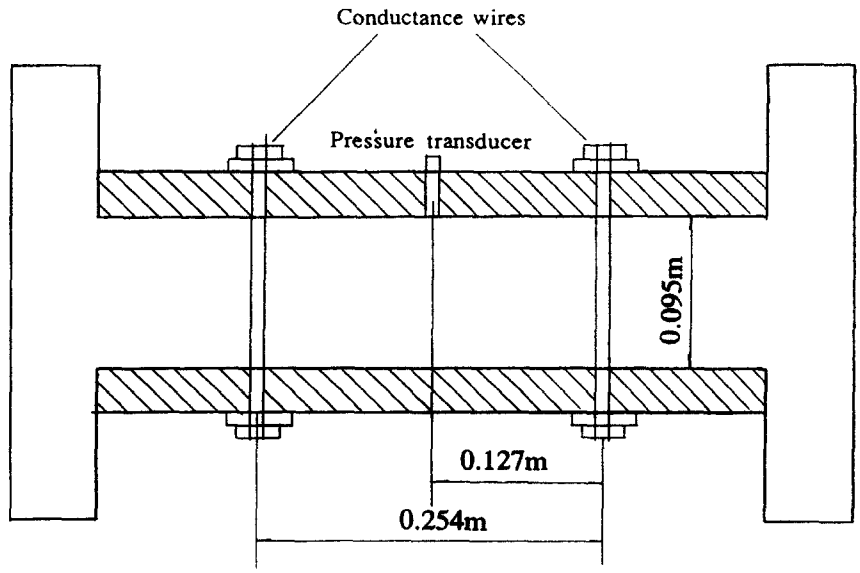

Figure 4. Test section.

4. RESULTS

4.1. Profile of the Pressure Distribution

Based on the model suggested in the theory for a stable slug, the ideal pressure distribution inside a slug is that shown in figure 5. In the front of the slug there is a sudden pressure increase due to the hydraulic jump. Then the pressure will increase gradually due to the friction at the pipe wall. There is another jump in pressure at the rear of the slug which is described by [7], [12] and [16]. This second jump in pressure could be much smaller than the first. After the slug moves past the pressure transducer, the pressure behind slugs maintains a high value until the slug flows out of the pipe. The pressure will then drop very quickly if there are no other slugs between the measuring point and the pipe exit.

Figure 6 presents pressure and liquid holdup measurements for a stable slug passing the measuring station when the superficial velocities of the gas and liquid are, respectively, 1.10 and 0.6 m/s. (In all figures, H_L is the liquid holdup, defined as the fraction of the pipe cross-sectional area occupied by liquid, and P is a dimensionless pressure, defined as $\tilde{P}/\rho_L g D$.) The arrival and the departure of the slug are indicated by a sudden increase and a sudden decrease in the conductance. From the measurement of the time for the slug to move the distance between two pairs of probes a slug velocity of $C_F = 2.07$ m/s is calculated. From this velocity and the length of time that the slug is detected by the conductance probes a slug length of about 1.65 m is obtained.

Values of ΔP_r, ΔP_f and ΔP_h estimated from the measurements are indicated. The pressure profile is qualitatively in agreement with the theoretical model, as can be seen from the values of $(\Delta P_h)_{th}$, $(\Delta P_f)_{th}$ and $(\Delta P_r)_{th}$ indicated in the figure. Sudden pressure increases are observed both at the front and rear of the slug, and there is a slow increase as the body of the slug passes. It is noted that

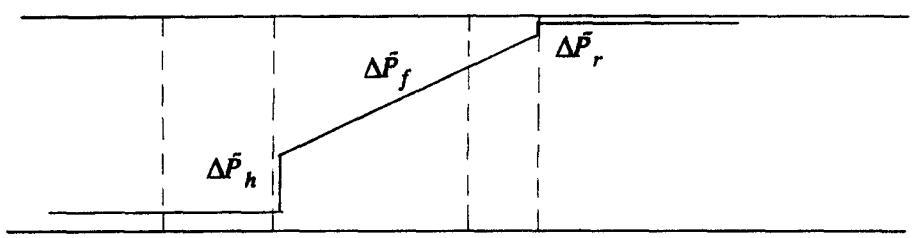

Figure 5. Idealized pressure profile for a stable slug.

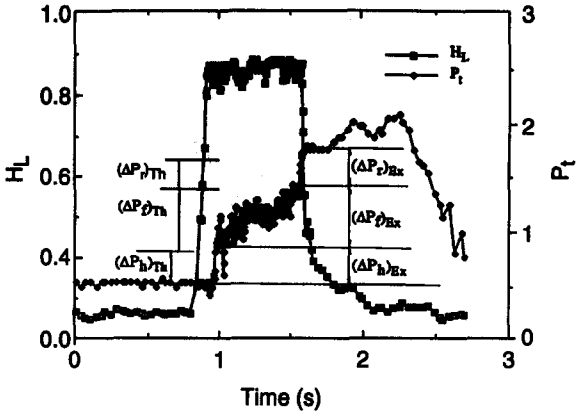

Figure 6. Pressure distribution for a stable slug at $u_{SG} = 1.10$ m/s, $u_{SL} = 0.6$ m/s, where pressure is made dimensionless with $\rho_L g D$.

the increase in pressure does not occur as soon as the slug arrives. It is believed that the product of this delay time and the slug velocity is roughly equal to the length of the circulating zone in front of the slug, in this case, roughly 0.12 m (1.3 times the pipe diameter).

Figures 7 and 8 show profiles for stable slugs at $u_{SG} = 2.96$ m/s and $u_{SG} = 4.06$ m/s. The same general pattern, as shown in figure 6, for $u_{SG} = 1.10$ m/s is noted. However, the pressure changes in the body of the slug are observed to be much more irregular. If u_{SG} is increased beyond 6 m/s, it is difficult to see the pressure increase in the rear of a stable slug, but the pressure increase in the front is quite evident. This is illustrated with the profiles shown in figure 9 for $u_{SG} = 7.03$ m/s and $u_{SL} = 0.9$ m/s and in figure 10 for $u_{SG} = 9.09$ m/s and $u_{SL} = 0.6$ m/s. The velocity of the slug front in figure 10 is measured as 13.19 m/s. The theoretical calculations of a dimensionless pressure increase of 10.74 in the front is to be compared with a measured value of about 10.

Figure 11 gives measurements of the liquid holdup obtained from two pairs of conductance probes separated by a distance of 0.254 m for $u_{SG} = 15.9$ m/s and $u_{SL} = 0.9$ m/s. The time scales of the two sets of measurements have been displaced so that they coincide at the front of the pattern. The open points represent measurements when the slug passed the upstream station, h_{L1}, and the filled points represent the downstream station, h_{L2}. These clearly show that the slug is increasing in size. A value of $(C_F - C_T) = 3.22$ m/s is calculated from the difference in the passing time indicated by the signals shown in figure 12 and the distance between the two probes. A value of $C_T = 15.83$ m/s was measured for the slug so that $(C_F - C_T)/C_T = 0.20$. The length is 1.4 m.

The pressure profile for this growing slug is shown in figure 12. An interesting feature is that there is a decrease in the pressure at the rear of the slug. This is consistent with [12] because the

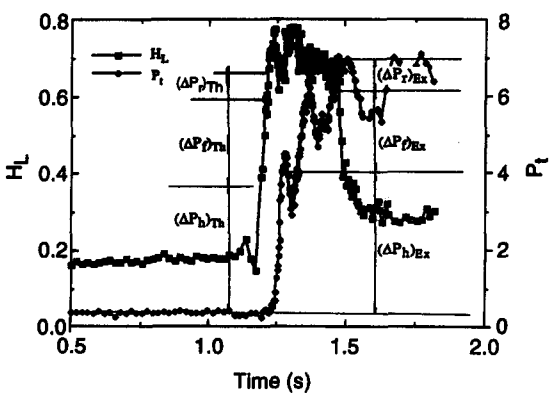

Figure 7. Pressure distribution for a stable slug at $u_{SG} = 2.96$ m/s, $u_{SL} = 0.9$ m/s, where pressure is made dimensionless with $\rho_L g D$.

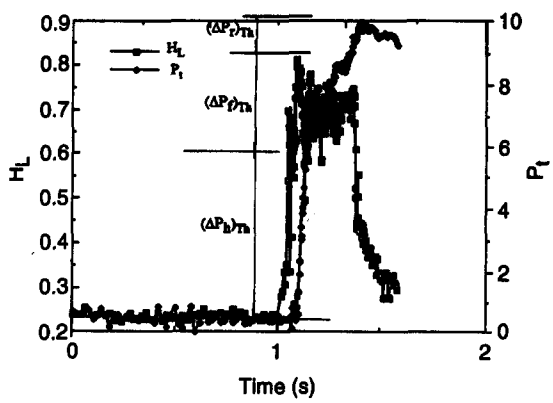

Figure 8. Pressure distribution for a stable slug at $u_{SG} = 4.06$ m/s, $u_{SL} = 0.5$ m/s, where pressure is made dimensionless with $\rho_L g D$.

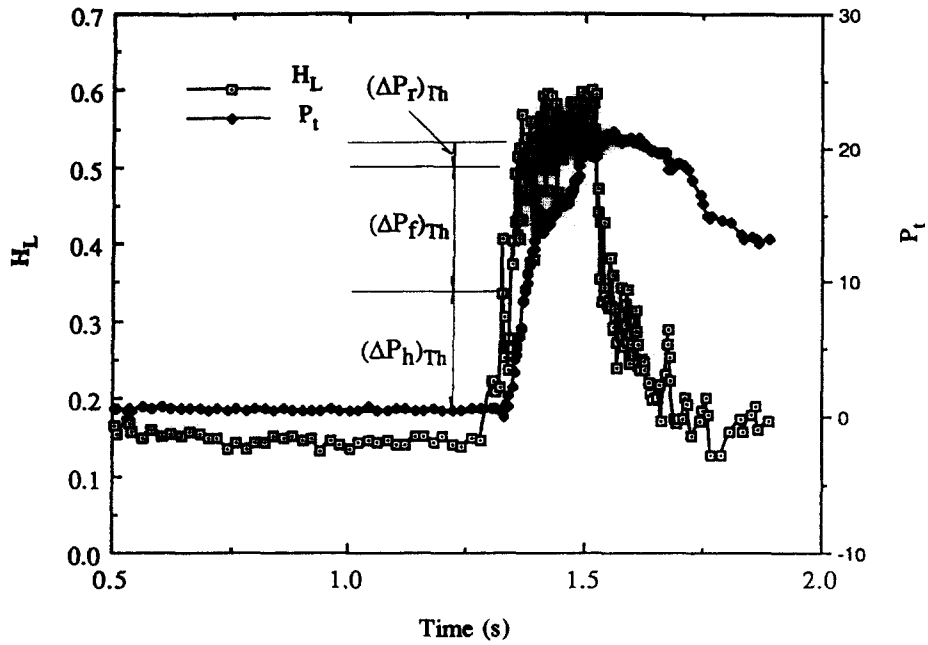

Figure 9. Pressure distribution for a stable slug at $u_{SG} = 7.03$ m/s, $u_{SL} = 0.9$ m/s, where pressure is made dimensionless with $\rho_L g D$.

top of the slug tail is not a stagnation point in a reference frame moving with C_F and there is actually an increase in the relative velocity from stations 4 to 5. Figures 13 and 14 show another example of a growing slug with a decrease in the pressure at the rear.

Figures 15 and 16 give measurements of liquid holdup and pressure for a decaying slug. The calculated pressure increase in the rear, shown in figure 16, is quite large because of the momentum change at the stagnation point and because of the momentum loss due to the contraction of the

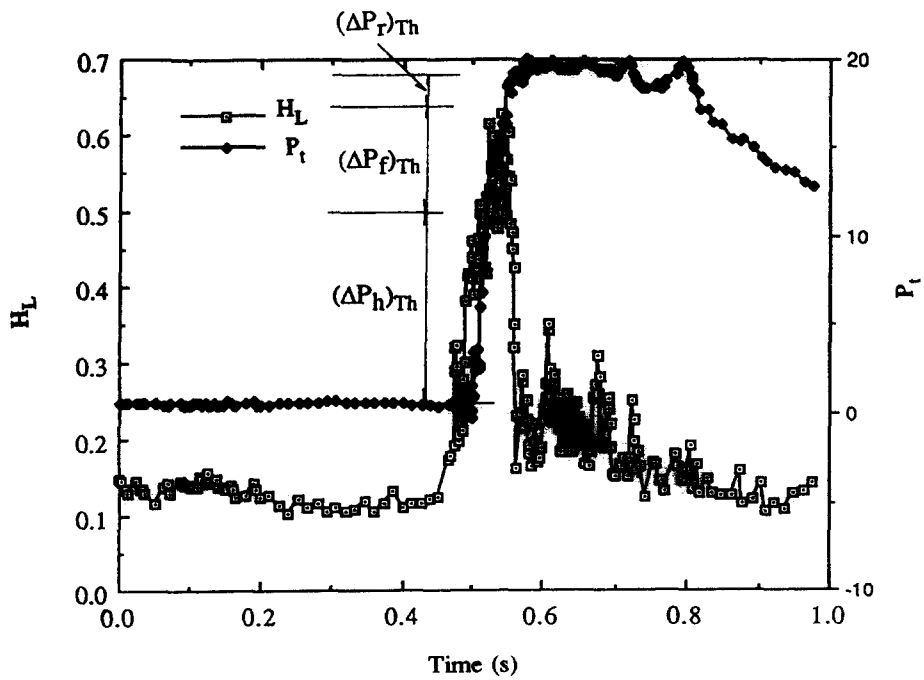

Figure 10. Pressure distribution for a stable slug at $u_{SG} = 9.09$ m/s, $u_{SL} = 0.6$ m/s, where pressure is made dimensionless with $\rho_L g D$.

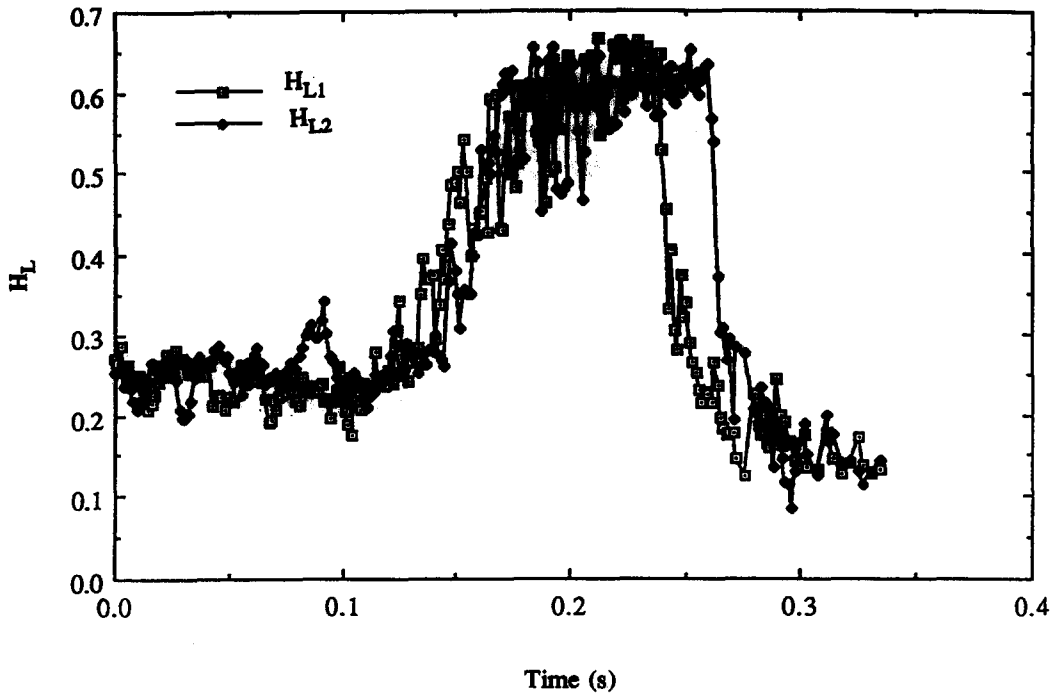

Figure 11. Liquid holdup for a growing slug at two locations for $u_{SG} = 15.9$ m/s, $u_{SL} = 0.9$ m/s. The probe at station 2 is downstream of the probe at station 1.

slug. An interesting aspect of the pressure profile shown in figure 16 is the large pressure minimum (of about 6.9×10^3 N/m^2) in the front of the slug. Similar minima can also be observed in figures 6, 9, 10, 12 and 14. These are probably associated with the vortical structure in front of the slugs, which controls aeration and becomes more intense as the gas velocity increases.

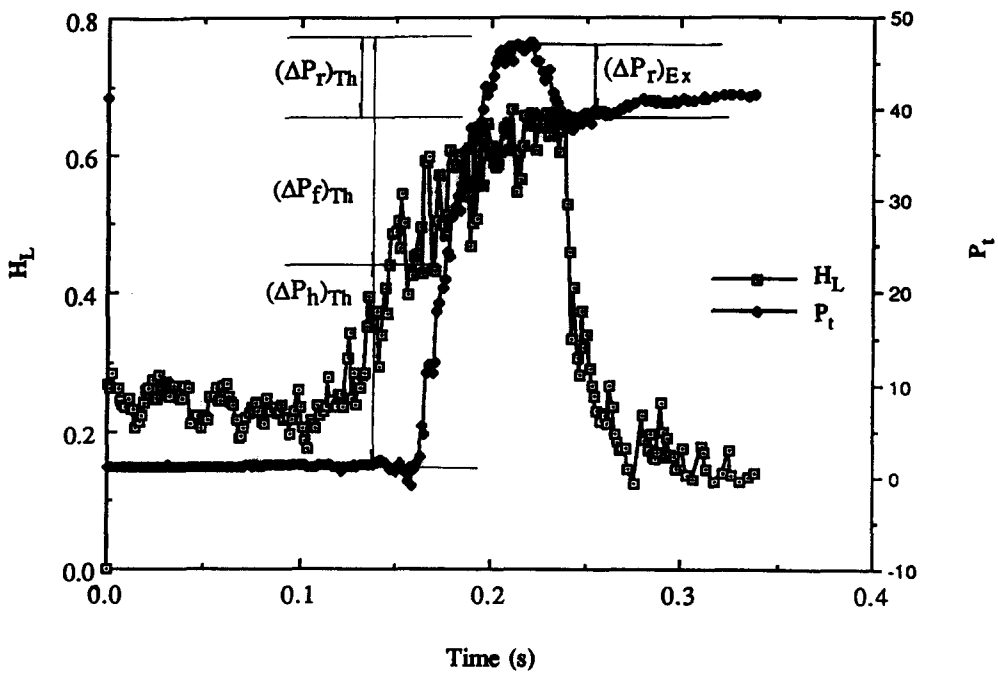

Figure 12. Pressure distribution for a growing slug at $u_{SG} = 15.9$ m/s, $u_{SL} = 0.9$ m/s, where pressure is made dimensionless with $\rho_L g D$.

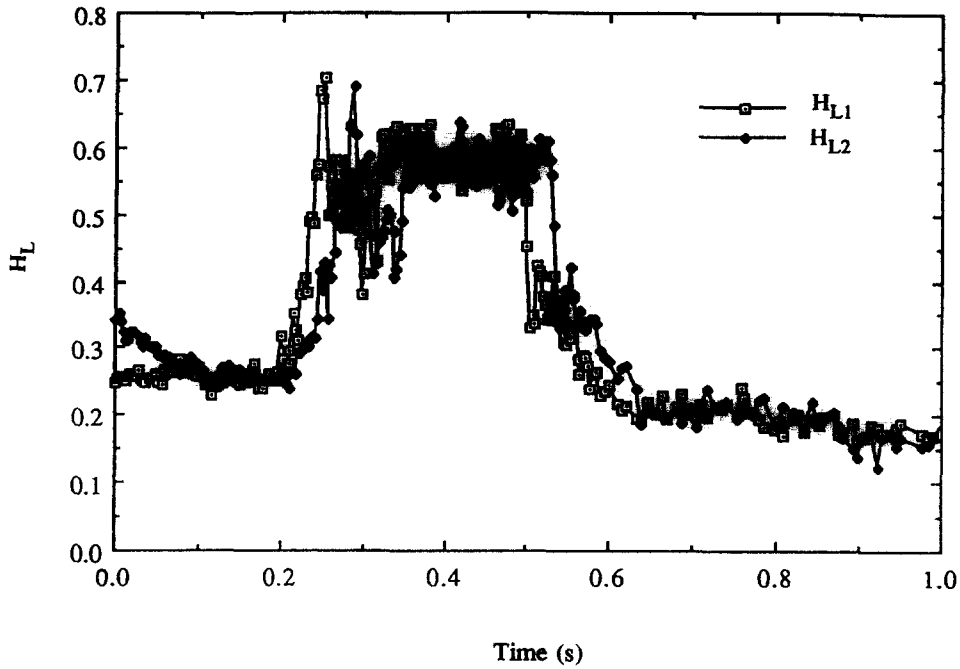

Figure 13. Liquid holdup for a growing slug at $u_{SG} = 7.03$ m/s, $u_{SL} = 0.9$ m/s. The probe at station 2 is downstream of the probe at station 1.

4.2. Quantitative Test of the Model

In making quantitative comparisons between measurements and the model equations it should be pointed out that the approximation of $(C_F - u_{L1})$ by C_F can lead to significant errors. For example, when $u_{SG} > 3$ m/s, the pressure increase at the hydraulic jump, ΔP_h, can be overestimated by as much as 10–40%. For the slug in figure 10, $C_F = 13.194$ m/s, u_{L1} is calculated to be 1.08 m/s, the error would be 17%.

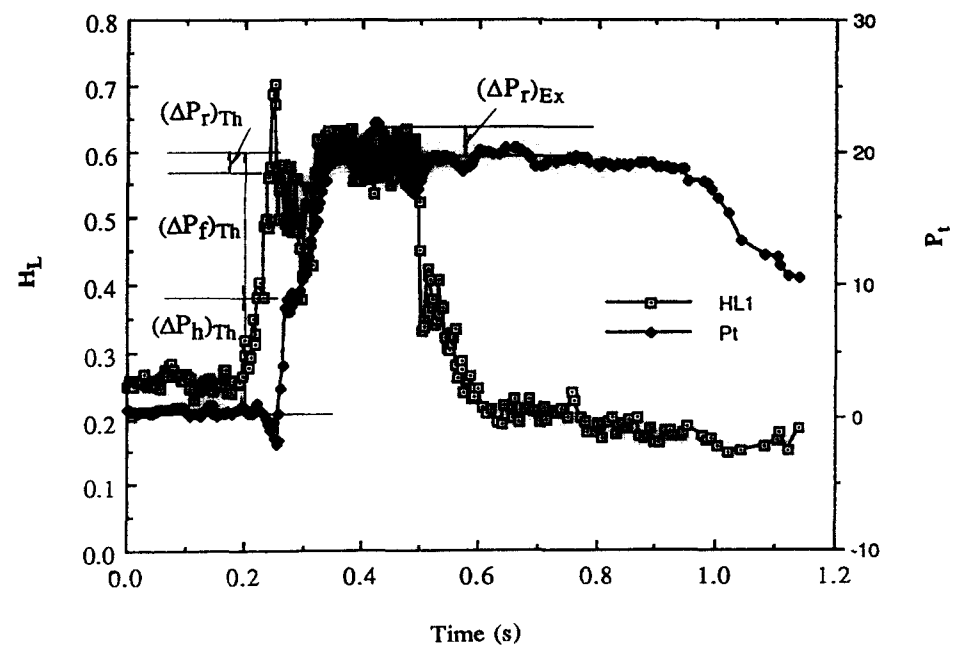

Figure 14. Pressure distribution for a growing slug at $u_{SG} = 7.03$ m/s, $u_{SL} = 0.9$ m/s, where pressure is made dimensionless with $\rho_L g D$.

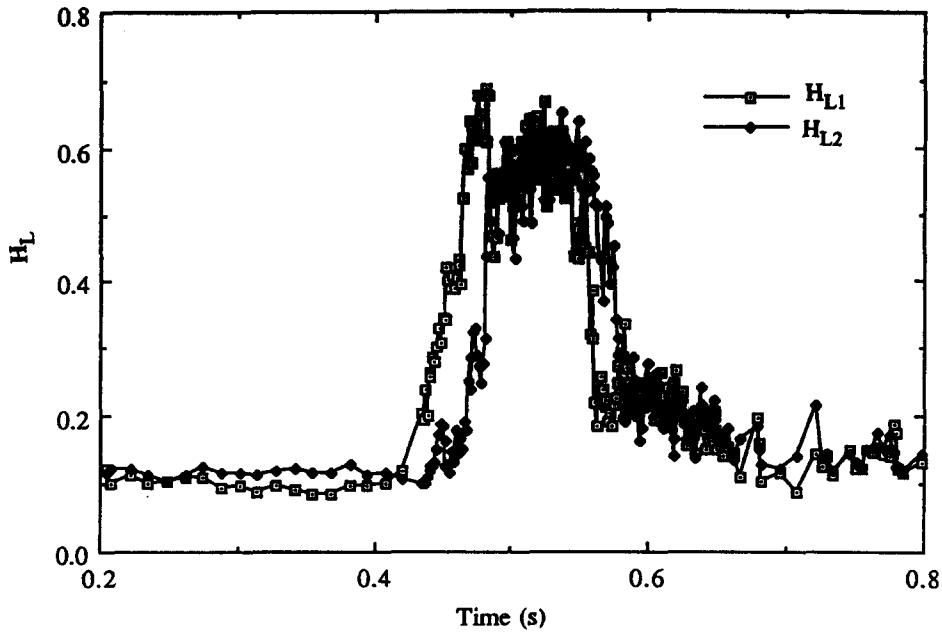

Figure 15. Liquid holdup for a decaying slug at $u_{SG} = 13.2$ m/s, $u_{SL} = 0.8$ m/s. The probe at station 2 is located downstream of the probe at station 1.

Similar errors can be made in calculating $\Delta\tilde{P}_f$, which varies as $u_{L3}^{1.8}$ if C_F is used to approximate u_{L3}. Typically this error is higher than 20% and, when $u_{SG} < 1.5$ m/s, it can be $> 50\%$. For the slug shown in figure 5, $C_F = 2.25$ m/s, $u_{L3} = 1.73$ m/s and $(C_F^{1.8} - u_{L3}^{1.8})/u_{L3}^{1.8} = 0.60$.

Values of $(\Delta\tilde{P}_h/\rho_L gD)$, $(\Delta\tilde{P}_f/\rho_L gD)$ and $(\Delta\tilde{P}_r/\rho_L gD)$ of 0.26, 0.71, 0.29 and 0.34, 0.58, 0.32 are calculated for the stable slugs shown in figures 6 and 7. The comparison between these calculated values and the measurements in these figures indicates good agreement. For higher u_{SG} it is difficult to differentiate the components of the pressure drop. However, the comparison given in figures 8–10 indicates a consistency between the measured and calculated pressure profiles.

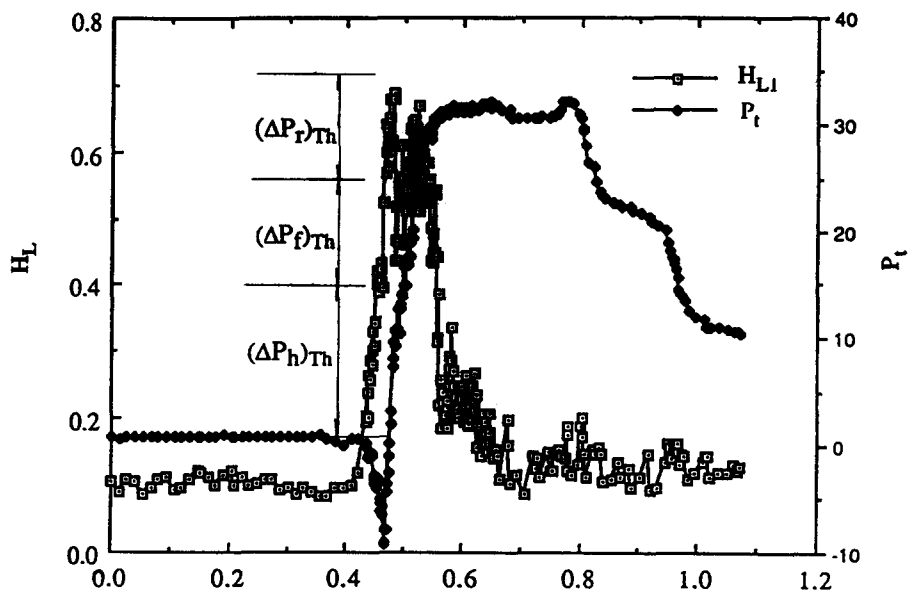

Figure 16. Pressure distribution for a decaying slug at $u_{SG} = 13.2$ m/s, $u_{SL} = 0.8$ m/s, where pressure is made dimensionless with $\rho_L gD$.

Table 1. Pressure drop over stable slugs (in this table, ΔP stands for $\Delta\tilde{P}/\rho_L gD$ and velocities are given in units of m/s)

u_{SG}	u_{SL}	C_F	ΔP_h	ΔP_f	ΔP_r	$(\Delta P_T)_{Th}$	$(\Delta P_T)_{EX}$
1.109	0.60	2.07	0.29	0.64	0.19	1.12	1.23
1.994	0.50	4.09	1.59	1.53	0.27	3.39	3.23
1.994	0.60	3.73	1.59	1.55	0.38	3.52	4.05
1.994	0.60	3.73	1.73	1.48	0.50	3.71	4.53
1.994	0.70	3.80	1.76	1.53	0.43	3.72	3.87
2.965	0.60	4.35	2.19	2.02	0.64	4.85	5.21
2.965	0.60	4.94	2.43	2.45	0.25	5.13	5.56
2.965	0.90	5.96	3.20	2.39	0.51	6.10	6.43
4.060	0.50	6.33	4.36	2.55	0.81	7.72	8.07
4.060	0.50	6.53	5.22	3.22	1.38	9.81	9.26
4.060	1.00	6.60	5.18	4.20	1.22	10.60	11.21
4.985	0.60	8.17	7.23	3.46	1.29	11.98	11.19
5.976	0.70	7.60	4.30	4.51	0.83	9.64	9.16
7.036	0.60	9.02	8.72	1.52	4.03	14.27	13.90
7.036	0.60	9.74	5.66	6.60	0.85	13.10	15.45
7.036	0.90	10.92	8.60	9.49	1.45	19.53	19.97
9.087	0.60	13.19	10.74	6.09	1.70	18.53	19.01
9.087	0.90	15.88	14.06	8.98	1.90	24.93	23.38
13.18	0.80	17.27	15.09	12.80	0.58	28.47	28.55
13.18	0.90	18.45	18.29	11.97	2.45	32.72	30.67
15.93	0.80	17.27	12.02	17.44	1.22	30.67	34.50
15.93	1.00	18.36	12.16	23.79	0.95	36.90	40.57

A sample listing of calculated pressure components for stable slugs is given in table 1. In many of the runs the measured components of the pressure drop were not as easily discerned as in the figures. Consequently, only the total dimensionless pressure drop, ΔP_T, is listed. It is noted that calculated ΔP_T are in good agreement with the measurements. When $u_{SG} = 1.10$ m/s, $\Delta\tilde{P}_f \gg \Delta\tilde{P}_h$ or $\Delta\tilde{P}_r$. The reason for this is that at low gas velocities the slug can be quite long, typically 1.5–3.5 m in the pipeline used in these experiments. Also, at low gas velocities, $\Delta\tilde{P}_r$ can be as large as $\Delta\tilde{P}_h$. When $u_{SG} > 2$ m/s the pressure drop at the rear of the slug, $\Delta\tilde{P}_r$, makes a small contribution to the total pressure drop. However, $\Delta\tilde{P}_f$ is still large and, for very long slugs, could be larger than $\Delta\tilde{P}_h$. As the gas velocity decreases, $\Delta\tilde{P}_h$ decreases. It was suggested by Fan *et al.* (1991) that when $\Delta\tilde{P}_h = 0$, the vortical structure disappears and a transition from slug to plug flow occurs.

Not many growing slugs were observed, possibly because the pipe was long enough for a fully developed condition to be reached. For the growing slug in figure 11, a cross-correlation analysis gives $C_F = 19.05$ m/s and $C_T = 15.83$ m/s. The calculated $(\Delta\tilde{P}_h/\rho_L gD)$, $(\Delta\tilde{P}_f/\rho_L gD)$ and $(\Delta\tilde{P}_r/\rho_L gD)$ of 23.40, 25.31 and -8.87 are compared to the measured pressure profile in figure 12. For the growing slug shown in figure 13, values of $C_F = 9.77$ m/s and $C_T = 8.50$ m/s were obtained. Calculated $(\Delta\tilde{P}_h/\rho_L gD)$, $(\Delta\tilde{P}_f/\rho_L gD)$ and $(\Delta\tilde{P}_r/\rho_L gD)$ values of 8.46, 10.3 and -1.25 are compared with measurements in figure 14. Good agreement between the calculations and the measurements is noted both in figures 12 and 14. In fact, the calculated total pressure drops $(\Delta\tilde{P}_T/\rho_L gD)$ of 39.84 and 17.54 agree, as well as can be expected, with measurements of 38.40 and 18.85.

Table 2. Pressure drop over decaying slugs (in this table, ΔP stands for $\Delta\tilde{P}/\rho_L gD$ and velocities are given in units of m/s)

u_{SG}	u_{SL}	C_F	C_T	ΔP_h	ΔP_f	ΔP_r	$(\Delta P_T)_{TH}$	$(\Delta P_T)_{EX}$
1.109	0.90	2.47	2.88	1.32	0.20	0.62	2.14	2.01
2.965	0.60	4.58	4.84	2.69	1.31	0.82	4.82	5.36
2.965	0.60	5.07	6.79	3.98	1.09	1.98	7.05	8.11
2.965	1.00	4.73	5.90	4.64	2.10	2.94	9.68	8.74
4.985	0.90	6.01	7.82	7.59	1.70	5.44	14.73	15.33
8.069	0.80	10.33	11.87	8.69	6.10	4.83	19.62	18.65
11.04	0.60	7.06	9.96	8.87	1.51	10.53	20.91	22.57
11.04	0.90	11.52	14.27	14.03	7.90	10.24	31.37	27.23
13.18	0.50	12.92	15.44	12.52	10.97	8.01	31.24	28.56
13.18	0.60	15.83	16.24	13.51	8.41	2.39	24.31	26.27
13.18	0.80	13.57	16.50	14.27	9.88	9.90	34.05	28.56
13.18	0.80	15.06	16.50	15.00	7.75	6.34	29.08	30.75
15.93	0.60	13.61	16.27	10.87	6.36	8.98	26.21	28.37
15.93	0.80	13.77	17.79	14.54	6.79	15.13	36.36	35.67

A large number of decaying slugs were observed. Comparisons of calculated and measured pressure drops are given in table 2. Again good agreement is found. It is noted, for decaying slugs, that $\Delta\tilde{P}_r$ can be large and of the same magnitude as $\Delta\tilde{P}_h$. For the decaying slug shown in figures 15 and 16, values of $C_F = 13.57$ m/s and $C_T = 16.50$ m/s are obtained. The calculated $(\Delta\tilde{P}_h/\rho_L gD)$, $(\Delta\tilde{P}_f/\rho_L gD)$ and $(\Delta\tilde{P}_r/\rho_L gD)$ of 14.27, 9.88 and 9.90 are indicated on the pressure profile shown in figure 16. The calculated and measured $(\Delta\tilde{P}_T/\rho_L gD)$ are 34.1 and 30.8.

4.3. Average Pressure Drop over Slugs

For a given flow condition a large variation of the pressure drop over individual slugs is found. The calculations show that these variations are associated, primarily, with variations of the height of the liquid in front of the slug and of the length of the slug. If a slug catches up with a decaying slug, the liquid layer in front of it becomes very thick. As a consequence, its length will increase rapidly. The increase in length causes an increase in the frictional pressure drop. The increase in h_{L1} causes an increase in ΔP_h because of an increase in the term

$$\left[\frac{A_{L1}}{A_3} - \left(\frac{A_{L1}}{A_3}\right)^2 (1-\epsilon_3)\right]$$

appearing in [6], [11] and [15].

Figure 17 gives averages of the pressure drop over slugs observed for different flow conditions. This average pressure drop increases with u_{SG} because C_F increases strongly with u_{SG}. However, for high u_{SG}; the average pressure drop increases with increasing u_{SL}.

5. DISCUSSION

This paper presents much needed measurements of the variation of pressure associated with the passage of stable or unstable slugs in a horizontal flow. Good agreement is obtained with a model which considers the overall pressure drop as the sum of contributions associated with a hydraulic jump in the front of the slug, a wall drag in the body of the slug and the sudden change in the velocity field in the rear of the slug. The pressure change in the rear, which seems to have been overlooked by previous investigators, can make a significant contribution.

The chief problem in developing the model is accounting for the influence of entrained gas. The agreement between experiment and calculation is as good as could be expected, considering the simplifying assumptions that were made. In analyzing the hydraulic jump, the bubbles in the slug body were assumed to be uniformly distributed and to be moving with the liquid velocity. Friction factor relations for single-phase flow were used to calculate the frictional pressure loss in the body of the slug. The effect of voidage is taken into account only by considering its role in increasing the liquid velocity.

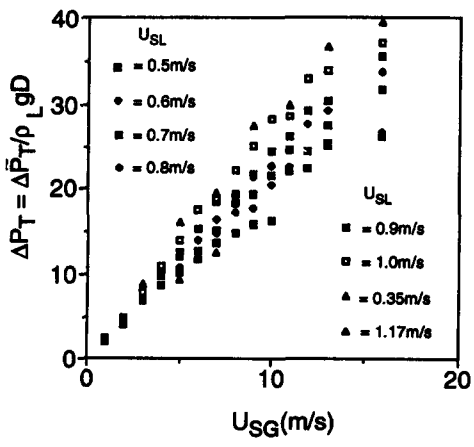

Figure 17. Average pressure drop over slugs.

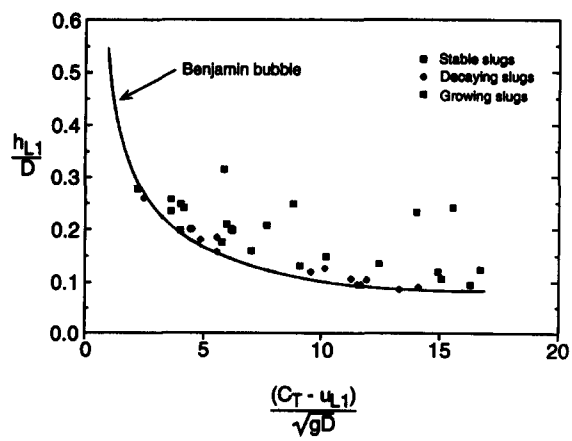

Figure 18. Conditions for the existence of slugs.

The treatment of the pressure change at the rear involved a drastic idealization. The measured pressure change along the top of the slug at the rear was pictured to be associated with an abrupt change in the liquid velocity, which could be modelled with the Bernoulli equation. In a stable slug the idealized flow looks like a stagnation point to an observer moving with the slug. Again, the influence of voidage is taken into account only insofar as it affects the liquid velocity. The success of this model at both high and low gas flows is surprising considering the highly erratic appearance of the tail caused by the ejection of air bubbles and the observed non-uniform distribution of voids. For example, the translational velocity of the slug in figure 6 is small and the bubbles concentrated near the top of the pipe at the rear of the slug. Figure 12 gives results for a growing slug that is moving with a high velocity. In this case the bubbles tend to be distributed uniformly along the whole slug length and the average void fraction is >0.3.

For stable slugs the pressure drop at the rear of the slug is small compared to the pressure drop due to the hydraulic jump and the wall drag. However, for unstable slugs, the pressure change at the rear can be as large as the other two components.

An important factor in determining whether a slug will grow or decay is the height of the liquid layer in front of the slug. Figure 18 presents measurements of the height of the liquid layer in front of the slug. The curve represents the necessary conditions for the existence of slugs suggested by Ruder *et al.* (1989). It is noted that slugs grow when h_{L1}/D is much larger than the necessary condition. The decaying slugs represented in this figure had h_{L1}/D approximately equal to the necessary condition. When a slug is closely behind a stable slug, the liquid layer in front of this slug could be very thin. The slug might not be able to pick up enough liquid to balance the liquid shed at the tail, so it will decay. When a slug is catching another which is collapsing, the liquid layer in front becomes thick. The slug will grow very quickly.

Acknowledgement—This work was supported by the Department of Energy under Grant DOE DEF GO2-86ER 13556.

REFERENCES

ANDRITSOS, N. & HANRATTY, T. J. 1987 Influence of interfacial waves in stratified gas–liquid flows. *AIChE Jl* **33,** 444–454.

BEGGS, H. D. & BRILL, J. P. 1973 A study of two-phase flow in inclined pipes. *J. Petrol. Technol.* **May,** 607–617.

BENJAMIN, T. B. 1968 Gravity currents and related phenomena. *J. Fluid Mech.* **31,** 209–248.

BONNECAZE, R. H., ERSKINE, J. R. & GRESKOVICH, E. J. 1971 Holdup and pressure drop for two-phase slug flow in inclined pipelines. *AIChE Jl* **17,** 1109.

CROWLEY, C. J. 1989 Scaling of multiphase flow at large pipe size and high gas density. Presented at the *4th Int. Conf. on Multiphase Flow*, Nice, France.

DUKLER, A. E. & HUBBARD, M. G. 1975 A model for gas–liquid slug flow in horizontal and near horizontal tubes. *Ind. Engng Chem. Fundam.* **14,** 337–347.

FAN, Z., JEPSON, W. P. & HANRATTY, T. J. 1991 A model for stationary slugs. *Int. J. Multiphase Flow* **18,** 477–494.

GREGORY, G. A., NICHOLSON, M. K. & AZIZ, K. 1978 Correlation of the liquid volume fraction in the slug for horizontal gas–liquid slug flow. *Int. J. Multiphase Flow* **4,** 33–39.

KOKAL, S. L. & STANISLAV, J. F. 1989 An experimental study of two-phase flow in slightly inclined pipes—II. Liquid holdup and pressure drop. *Chem. Engng Sci.* **44,** 681–693.

LAURINAT, J. E., HANRATTY, T. J. & DALLMAN, J. C. 1984 Pressure drop and film height measurements for annular gas–liquid flow. *Int. J. Multiphase Flow* **10,** 341–356.

LIN, P. Y. & HANRATTY, T. J. 1986 Prediction of the initiation of slugs with linear stability theory. *Int. J. Multiphase Flow* **12,** 79–98.

LIN, P. Y. & HANRATTY, T. J. 1987 Detection of slug flow from pressure measurements. *Int. J. Multiphase Flow* **13,** 13–21.

RUDER, Z. & HANRATTY, T. J. 1990 A definition of gas/liquid plug flow in horizontal pipes. *Int. J. Multiphase Flow* **16,** 233–242.

RUDER, Z., HANRATTY, P. J. & HANRATTY, T. J. 1989 Necessary conditions for the existence of stable slugs. *Int. J. Multiphase Flow* **15**, 209–226.

SINGH, G. & GRIFFITH, P. 1970 Determination of the pressure drop optimum pipe size for a two-phase slug flow in an inclined pipe. *TASME Jl Engng Ind.* **92**, 717–726.

WEISMAN, J., DUNCAN, D., GIBSON, J. & CRAWFORD, T. 1979 Effects of fluid properties and pipe diameter on two-phase flow patterns in horizontal lines. *Int. J. Multiphase Flow* **5**, 437–462.